

Study of symmetry and disordering of Si(111)-7×7 surfaces by optical second harmonic generation

T. F. Heinz, M. M. T. Loy, and W. A. Thompson
IBM T. J. Watson Research Center, Yorktown Heights, New York 10598

(Received 15 February 1985; accepted 18 April 1985)

A detailed study of the polarization dependences of the second-harmonic generation process from clean Si(111)-7×7 surfaces is presented and analyzed in terms of the symmetry properties of the surface. Results from real-time, *in situ* measurements on disordering of the Si(111)-7×7 surface by oxidation and Ar⁺ ion bombardment are also reported.

I. INTRODUCTION

The process of optical second-harmonic generation (SHG) from a centrosymmetric medium has been found to be highly sensitive to the character of its surface on an atomic level. This behavior arises from the fact that SHG is (electric-dipole) forbidden within the bulk of a centrosymmetric material, but is allowed in the surface region where the inversion symmetry is broken. Indeed, fractional monolayers of atomic^{1,2} and molecular² adsorbates can be detected readily by SHG measurements. The SH technique has already proved useful for studying the spectroscopy³ and orientation⁴ of adsorbed molecules. Recently, we have demonstrated that the technique can also be applied to probe the symmetry of ordered crystalline surfaces through the polarization dependences of the surface SHG process.⁵ For the case of clean Si(111) surfaces, the SH signals from the 2×1 and 7×7 reconstructions could be distinguished from one another and analyzed in terms of their differing symmetry properties. In this paper, we present a detailed discussion of the polarization dependences of the SHG process for the Si(111)-7×7 surface and report new results on the disordering of this surface induced by bombardment with energetic Ar⁺ ions. From our real-time measurements of the SH signal, we are able to infer a value for the average area of the surface disordered by each incoming ion. Data are also reported for the oxidation of the Si(111)-7×7 surface.⁶

II. EXPERIMENTAL

The Si(111)-7×7 surfaces were prepared and studied in a standard ion-pumped ultrahigh vacuum chamber at a base pressure of $\sim 5 \times 10^{-11}$ Torr. The surfaces were obtained by cleaving *in situ* a high purity silicon bar (doped with boron at 10^{-15} cm⁻³) along the $[2\bar{1}\bar{1}]$ direction. The 7×7 reconstruction resulted from a heating cycle bringing the sample to ~ 600 °C. Low-energy electron diffraction and Auger electron spectroscopy were applied to verify the surface structure and cleanliness of the samples. The pump radiation for the SH measurements was supplied by a Q-switched Nd:YAG laser operating at 1.06 μ m and producing 8 ns pulses at a 10-Hz repetition rate. The laser radiation was directed at normal incidence onto the sample surface, where the beam was lightly focused to a diameter of ~ 1 mm. The laser energy was always maintained sufficiently low to avoid any photoinduced changes in the surface. For a pump pulse of ~ 10 mJ energy, the reflected SH radiation typically consisted of $\approx 10^3$ photons. The SH signal was detected with a

photomultiplier and gated electronics after being isolated spectrally by means of color filters and a monochromator.

III. WELL-ORDERED SI(111)-7×7 SURFACES

For the Si(111)-7×7 surface, the SH intensity has been recorded as a function of the orientation of the linearly polarized pump electric field vector. The data for the intensity of the SH output polarized along the two orthogonal $[2\bar{1}\bar{1}]$ and $[0\bar{1}\bar{1}]$ surface crystal axes have been presented previously.⁵ In Fig. 1 we display the corresponding SH electric-field amplitude for the same two independent directions. The magni-

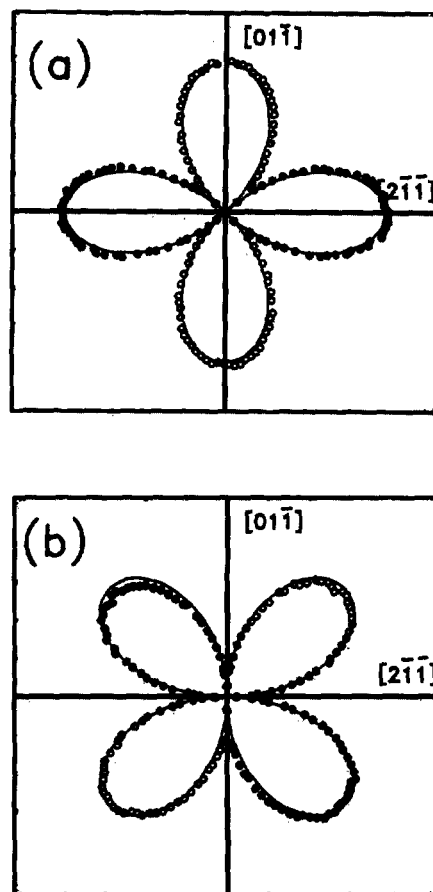


FIG. 1. SH electric field as a function of the angular orientation of the linearly polarized pump electric-field vector for a clean Si(111)-7×7 surface. The field amplitudes polarized along (a) the $[2\bar{1}\bar{1}]$ (x) direction and (b) the $[0\bar{1}\bar{1}]$ (y) direction. Open and filled points correspond to sign changes in the experimental data. The solid curves represent theoretical predictions for the magnitude of the SH electric field under $3m$ symmetry.

tude of the electric-field components is determined directly from the measured SH intensity, but the relative phase between them is not specified. To determine this relative phase, we examined data collected for the SH intensity with the output polarizer oriented midway between the two orthogonal axes, i.e., along the $[10\bar{1}]$ direction. From these data, we found that the SH electric field was linearly polarized. The changes in the relative phase of the two components indicated in Fig. 1 correspond to a smooth variation in the polarization of the SH radiation as the pump polarization is rotated. The open and filled points in the figure correspond to 180° phase differences in the electric-field amplitude.

The data in Fig. 1 completely characterize the SH electric field for any given polarizations of the pump laser. Consequently, we can transform these results into plots of the SH electric field components lying parallel and perpendicular to the polarization vector of the pump beam. This formulation of the experimental data reflects more directly the symmetry of the surface, since the curves can be viewed as having been obtained either by a rotation of the input and output polarizers with a sample fixed in space or, equivalently, by a rotation of the sample about its surface normal with fixed polarizers. Figure 2(a) displays the SH electric field polarized parallel to the pump polarization; Figure 2(b) corresponds to the orthogonal component of the SH field.

We now turn to the analysis of the polarization dependences of Figs. 1 and 2. We should first note that the SH

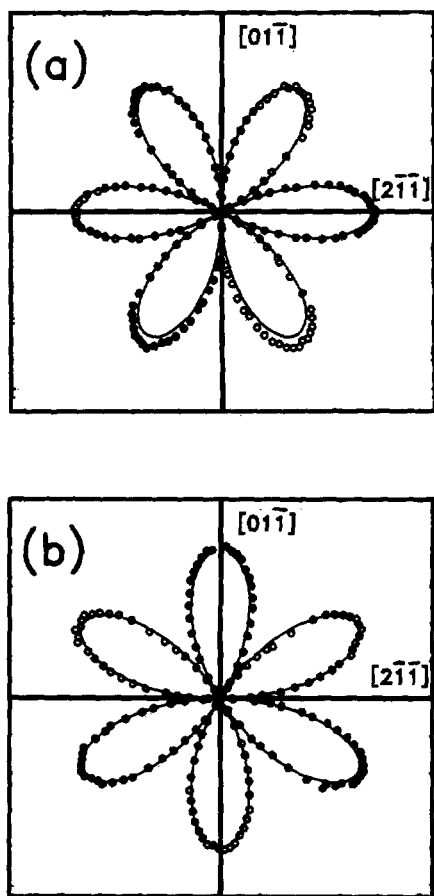


FIG. 2. As in Fig. 1, but with the SH electric field resolved along directions (a) parallel and (b) perpendicular to the pump electric-field vector.

signal for our experimental conditions appears to be dominated by the surface contribution. The effect of the symmetry-allowed higher-order (magnetic-dipole and electric-quadrupole) terms is insignificant. This statement is justified by the results for the oxidation of the silicon surface discussed below. In order to analyze the form of the surface contribution to the SH signal, we introduce the third-rank surface nonlinear susceptibility tensor $\vec{\chi}_s^{(2)}$ relating the induced nonlinear dipole moment per unit area and the pump electric-field vector in the surface layer:

$$\mathbf{P}_s^{\text{NLS}}(2\omega) = \vec{\chi}_s^{(2)} : \mathbf{E}(\omega) \mathbf{E}(\omega). \quad (1)$$

This relation takes account of the entire nonlinear source (NLS) polarization in the surface layer and does not presuppose that only the electric-dipole terms in a multipole expansion are important. Formal expressions for $\vec{\chi}_s^{(2)}$ can be derived from second-order perturbation theory, and a complete equation for the amplitude of the electric field of the reflected SH beam can be obtained by solving the wave equation for the specified nonlinear source term. Here we shall restrict our attention to the polarization dependences of the SHG process, which reflect the tensor properties of $\vec{\chi}_s^{(2)}$ and, hence, the symmetry properties of the surface. The strength of the radiated SH field polarized along the direction $\hat{e}(2\omega)$ is given by

$$\mathbf{E}(2\omega) \cdot \hat{e}(2\omega) = C \hat{e}(2\omega) \cdot \vec{\chi}_s^{(2)} : \hat{e}(\omega) \hat{e}(\omega), \quad (2)$$

where $\hat{e}(\omega)$ is the polarization vector of the pump electric field and C is a constant independent of the input and output polarization vectors. For a specified form of the surface nonlinear susceptibility tensor, this equation permits one to predict any desired polarization dependence.

The data in Fig. 2 suggest immediately that the Si(111)- 7×7 surface possesses a threefold rotational symmetry about its surface normal. The presence of the null values in Fig. 2(a) indicates additional symmetries in the Si(111)- 7×7 surface. For the input and output polarizations parallel to one another, the SHG process will be forbidden if this common direction lies perpendicular to a mirror plane. This situation is effectively a one-dimensional form of inversion symmetry. Examining Fig. 2(a), we find a mirror plane parallel to the $[2\bar{1}\bar{1}]$ crystal axis and two other mirror planes at $\theta = \pm 120^\circ$. Thus, the full symmetry of the Si(111)- 7×7 surface appears to be $3m$, just as would be the case for the ideal, unreconstructed Si(111) surface. Under $3m$ symmetry $\vec{\chi}_s^{(2)}$ has only a single independent, nonvanishing element: $[\chi_s^{(2)}]_{xxx} = -[\chi_s^{(2)}]_{xyy} = -[\chi_s^{(2)}]_{yxy}$, where x and y correspond, respectively, to the $[2\bar{1}\bar{1}]$ and $[0\bar{1}\bar{1}]$ directions in the crystal surface.

With the form of $\vec{\chi}_s^{(2)}$ appropriate for $3m$ symmetry, we can apply Eq. (2) to derive expressions for the radiated SH electric field. For the x and y components, we obtain

$$\begin{aligned} E_x &= C [\chi_s^{(2)}]_{xxx} \cos 2\theta, \\ E_y &= -C [\chi_s^{(2)}]_{xxx} \sin 2\theta, \end{aligned} \quad (3)$$

where the angle θ denotes the orientation of the pump polarization with respect to the $[2\bar{1}\bar{1}]$ axis (increasing towards the $[0\bar{1}\bar{1}]$ axis). The corresponding relations for the electric-field amplitudes parallel and perpendicular to the pump polariza-

tion are

$$\begin{aligned} E_{\parallel} &= C [\chi_s^{(2)}]_{xxx} \cos 3\theta, \\ E_{\perp} &= -C [\chi_s^{(2)}]_{xxx} \sin 3\theta. \end{aligned} \quad (4)$$

Here the polarization vector defining the parallel direction lies at an angle θ with respect to the $[2\bar{1}\bar{1}]$ axis; the vector for the perpendicular direction makes an angle of $\theta + 90^\circ$. One immediate result of Eq. (3) or Eq. (4) is the lack of any dependence in the total SH intensity (taking both polarizations together) on the pump polarization. For normally incident excitation on a surface with $3m$ symmetry, anisotropy can only be observed if the direction, rather than just the magnitude, of the radiated SH electric field is detected.

The solid lines in Figs. 1 and 2 represent the magnitude of the SH electric field predicted by Eqs. (3) and (4), respectively. The constant C has been adjusted to match the overall scale. The relative changes in sign in the electric-field amplitude (not shown) coincide with the experimental results. Good overall agreement is seen between the experimental data and the theoretical curves for $3m$ symmetry. As discussed above, the lack of SH signal for certain orientations in Fig. 2(a) indicates the presence of mirror planes. In order to verify more closely the existence of the mirror planes, we have performed direct measurement of the SH signal with parallel input and output polarizers oriented along and at $\pm 120^\circ$ from the $[01\bar{1}]$ axis. In this manner, we were able to place an upper bound of 3×10^{-3} on the intensity of these symmetry-forbidden signals compared with the symmetry-allowed signal obtained by removing the output polarizer. These results provide a rather sensitive check on the presence of three mirror planes. It should be noted that both resonant and nonresonant transitions can contribute to SHG and, consequently, a vanishing of the SH signal cannot be attributed to fortuitous symmetries of a particular state involved in the nonlinear process.⁷

It is instructive to compare linear and nonlinear optical measurements from a surface with $3m$ symmetry. As we have seen, the SHG process, described by a third-rank susceptibility tensor, reflects the anisotropic character of the surface. On the other hand, the linear response, characterized by a second-rank tensor, will be isotropic under $3m$ symmetry. Thus, only the nonlinear optical process permits one to distinguish between $3m$ and higher (e.g., isotropic) symmetry.

IV. DISORDERED Si(111)- 7×7 SURFACES

Before considering the question of the disordering of Si(111)- 7×7 surfaces, let us note a distinctive feature of the SHG process. For pump radiation striking the surface of a centrosymmetric medium at normal incidence, SH radiation from the surface is allowed only in the presence of ordering. This general result follows from symmetry arguments. For normally incident excitation, the electric field of the pump lies in the plane of the surface and only the component of the induced SH polarization in this same plane can contribute to the reflected SH radiation. Thus, the SHG process can occur only if there are nonzero components of the surface nonlinear susceptibility tensor with all three indices corresponding to directions in the surface plane. In the case of a surface with

isotropic symmetry (or inversion symmetry in the plane), these components must all vanish. Hence, surface SH radiation for our experimental geometry is correlated with the presence of ordering in the surface plane. More specifically, for measurements of the SH intensity with parallel input and output polarizers, the signal is associated with the lack of mirror symmetry normal to the chosen direction of polarization.

We now present SH measurements on the oxidation and ion bombardment of Si(111)- 7×7 surfaces. We were able to collect the data *in situ* and in real time, since the surface SHG technique can be applied in the presence of a gas and provides a sufficiently favorable signal-to-noise ratio to follow changes on the time scale of seconds. In the measurements discussed below, the input and output polarizations lay along the $[2\bar{1}\bar{1}]$ direction, which is not perpendicular to any mirror plane of the Si(111)- 7×7 surface.

First we report on the room-temperature oxidation of the Si(111)- 7×7 surface. In this experiment, the clean Si(111)- 7×7 surface was exposed to research grade oxygen at a pressure of 10^{-6} Torr. This led to a smooth fall in the SH signal to a very low level (Fig. 3). The decay in the SH radiation⁸ occurred for an exposure of ~ 100 L, which is sufficient to allow adsorption of roughly a monolayer of oxygen.⁹ This result clearly shows that the surface contribution to the SH signal for the clean Si(111)- 7×7 surface dominates that from the bulk for our experimental conditions. The decrease in the SHG efficiency can be attributed to the loss of long range ordering in the surface known to accompany the oxidation process.⁹ In addition to the change in symmetry, the SH susceptibility for the partially ordered surface may be diminished by an upward shift in the energy of the surface states as the dangling Si bonds are joined with oxygen atoms, causing the transitions between surface states in the SHG process to be further from resonance.

Ion bombardment of the silicon sample provides an interesting case for monitoring disordering. In this process, the change in the chemical composition of the surface is minor, but the change in the structure is pronounced. Figure 4 displays the SH intensity as a function of exposure to Ar^+ ions. The 5-keV ions struck the silicon sample at 45° from the surface normal with a flux of $2 \times 10^{11}/\text{cm}^2 \text{ s}$ measured in the surface plane. The theoretical fit in the figure was construct-

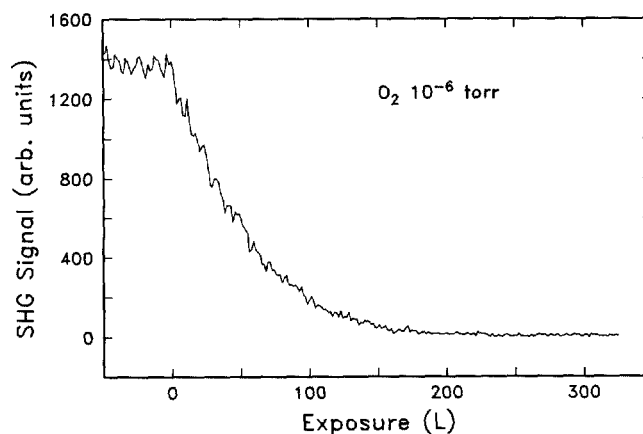


FIG. 3. SH intensity from a Si(111)- 7×7 surface during exposure to oxygen.

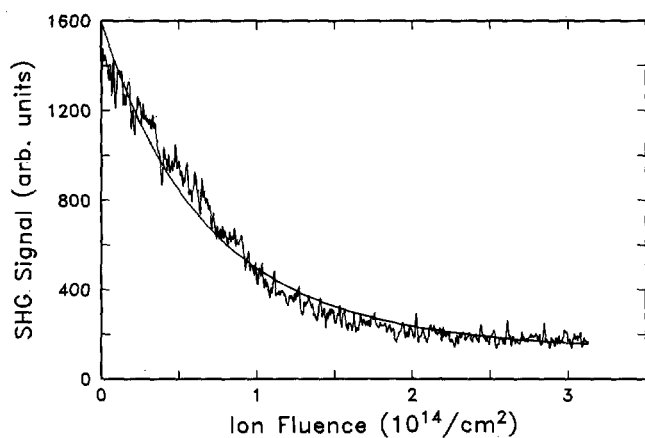


FIG. 4. SH intensity from a Si(111)- 7×7 surface measured during bombardment with 5-keV Ar^+ ions. The solid line represents the theoretical fit discussed in the text.

ed by assuming a surface nonlinear susceptibility that fell exponentially with increasing exposure, dropping to a small constant value associated with residual ordering. On the basis of this simple analysis, we can infer a value for the average effective area disordered by each incoming ion. From the parameters of the fit, we find this average area to be 105 \AA^2 .

A comparison of the effective area disordered by each ion with the corresponding sputtering yield helps to give a picture of the effect of the energetic ions. From the literature,¹⁰ we find that the sputtering yield of the 5-keV Ar^+ ions is ~ 1.5 . Thus, an average area of $\sim 70 \text{ \AA}^2$ is disordered for each ejected atom. This large area indicates that the ion bombardment process disorders many more atoms in the surface layer of the crystal than it ejects. Such behavior can be seen clearly in dynamical simulations of the ion bombardment process.¹¹

V. CONCLUSION

The surface second-harmonic technique appears to be a sensitive probe of the symmetry of the ordering of the top

atomic layers of a surface. The method is particularly well suited for identifying planes of mirror symmetry, which can be related to nulls in the surface SH signal. In the present work, this notion was applied in a precise measurement of mirror planes in the ideal Si(111)- 7×7 structure. SH measurements of the development of effective mirror planes also served to monitor disordering of the Si(111)- 7×7 surface induced by oxidation and ion bombardment. The capability of this method for performing real-time, *in situ* studies should be helpful in attacking a variety of problems involving structural changes of surfaces during the course of reactions.

This work was supported in part by the Office of Naval Research.

¹J.M. Chen, J.R. Bower, C.S. Wang, and C.H. Lee, *Opt. Commun.* **9**, 132 (1973).

²H. W. K. Tom *et al.*, *Phys. Rev. Lett.* **52**, 348 (1984), and references therein.

³T.F. Heinz, C. K. Chen, D. Ricard, and Y.R. Shen, *Phys. Rev. Lett.* **48**, 478 (1982).

⁴T.F. Heinz, H.W.K. Tom, and Y.R. Shen, *Phys. Rev. A* **28**, 1883 (1983).

⁵T.F. Heinz, M.M.T. Loy, and W.A. Thompson, *Phys. Rev. Lett.* **54**, 63 (1985).

⁶For SHG measurements of oxidized silicon samples under ambient conditions, see H.W.K. Tom, T.F. Heinz, and Y.R. Shen, *Phys. Rev. Lett.* **51**, 1983 (1983), and references therein.

⁷The $3m$ symmetry of the Si(111)- 7×7 surface is supported, with varying degrees of precision, by other surface probes, including low-energy electron diffraction, ion scattering, and scanning tunneling microscopy.

⁸In repeated trials of the oxidation measurements, we observed a variation in the rate of decay of the SH signal as a function of oxygen exposure. This behavior is presumably associated with differences in the surface defect density or low levels of surface contamination, both of which can strongly affect the oxidation process.

⁹B. Carriere and J. P. Deville, *Surf. Sci.* **80**, 278 (1979), and references therein.

¹⁰S. T. Kang, R. Shimizu, and T. Okutani, *Jpn. J. Appl. Phys.* **18**, 1717 (1979).

¹¹See, for example, R. P. Webb and D. E. Harrison, Jr., *Phys. Rev. Lett.* **50**, 1478 (1983).